Self-induced temperature gradients in Brownian dynamics

Jack Devine and M. W. Jack*

Department of Physics, University of Otago, Dunedin, New Zealand

Brownian systems often surmount energy barriers by absorbing and emitting heat to and from their local environment. Usually, the temperature gradients created by this heat exchange are assumed to dissipate instantaneously. Here we relax this assumption to consider the case where Brownian dynamics on a time-independent potential can lead to self-induced temperature gradients. In the same way that externally imposed temperature gradients can cause directed motion, these self-induced gradients affect the dynamics of the Brownian system. The result is a coupling between the local environment and the Brownian subsystem. We explore the resulting dynamics and thermodynamics of these coupled systems and develop a robust method for numerical simulation. In particular, by focusing on one-dimensional situations, we show that self-induced temperature gradients reduce barrier-crossing rates. We also consider a heat engine and a heat pump based on temperature gradients induced by a Brownian system in a nonequilibrium potential.

I. INTRODUCTION

Brownian dynamics on energy potentials has been used to describe colloidal particles [1] and also has had widespread application as a model for motor proteins [2–11], artificial nanodevices [12–17], and as a theoretical tool for understanding how thermodynamics manifests at the nanoscale [18–29]. The exchange of energy between the Brownian system and its environment is fundamental to the dynamics and thermodynamics of these systems. This is particularly apparent in the field of Brownian motors [30,31], where researchers have explored the dynamics and thermodynamics of isothermal Brownian systems converting energy between degrees of freedom [5,30–34] and Brownian systems absorbing energy from external temperature gradients [23,35] or two baths at different temperatures [29,34,36] to produce mechanical work. In this paper, we explore the thermodynamics and dynamics of a Brownian system coupled to its local environment. The Brownian system is coupled in such a way that due to heat exchanges with this environment, it creates temperature gradients which in turn influence its own behavior.

In this paper, we consider Brownian dynamics in the overdamped limit described by the Smoluchowski equation [1],

$$\partial_t P(\boldsymbol{r}, t) = -\boldsymbol{\nabla} \cdot \boldsymbol{J}(\boldsymbol{r}, t), \tag{1a}$$

$$J_j(\boldsymbol{r}, t) = -\gamma_j^{-1}[P(\boldsymbol{r}, t)\, \partial_j V(\boldsymbol{r}) + k_B T(\boldsymbol{r}, t)\, \partial_j P(\boldsymbol{r}, t)], \tag{1b}$$

where $P(\boldsymbol{r}, t)$ is the probability of finding the Brownian system at position $\boldsymbol{r}$ in configuration space (representing the state of the system) at time t, $\boldsymbol{J}(\boldsymbol{r}, t)$ is the probability current, and j is the index for each dimension. γ_j is the mobility of the Brownian system, k_B is Boltzmann's constant, and $T(\boldsymbol{r}, t)$ is the temperature of the environment. $V(\boldsymbol{r})$ is the *time-independent* potential experienced by the Brownian system and, in general, is nonconfining such that it drives the system out of equilibrium.

Isothermal Brownian systems, where $T(\boldsymbol{r}, t) = T_0$, have been considered by a number of authors [5,30–34]. One of the key characteristics of the dynamics of a Brownian system in a constant-temperature environment is that it absorbs heat from its environment to surmount energy barriers, reemitting this heat as it descends the barrier [26,27,37–39]. The heat flow per unit volume emitted by the system into its environment is given by [34]

$$q(\boldsymbol{r}, t) = -\boldsymbol{J}(\boldsymbol{r}, t) \cdot \boldsymbol{\nabla} V(\boldsymbol{r}). \tag{2}$$

In principle, this absorption and emission of heat produces temperature gradients in the local environment. By definition, these temperature gradients are not considered in cases where the temperature is a known function of time. Neglecting these self-induced temperature gradients is based on two implicit assumptions: first, that the environment dissipates temperature gradients much more rapidly than the dynamics of the Brownian system and, second, that the environment has a large enough heat capacity that any energy emitted into the environment has a negligible impact on the environmental temperature.

On the other hand, Büttiker and Landauer [23,35] have recognized that externally imposed temperature gradients, $\boldsymbol{\nabla} T(\boldsymbol{r}, t) \neq 0$, in the surrounding environment can significantly influence Brownian dynamics. In particular, an externally imposed temperature gradient can lead to net motion of a Brownian system against an external force, such that it acts as a heat engine. More recently, Brownian heat pump and refrigerator concepts based on this phenomena have been proposed [29,40].

In the current work, we explicitly consider the temperature gradients induced by the heat produced by a Brownian system via Eq. (2) and explore the impact of these gradients back on the Brownian dynamics. We do this by introducing an equation of motion for $T(\boldsymbol{r}, t)$, such that the probability density $P(\boldsymbol{r}, t)$ of the Brownian system is explicitly coupled to the local environmental temperature $T(\boldsymbol{r}, t)$. Noting the form of Eq. (2), we assume the equation of motion

$$\partial_t T(\boldsymbol{r}, t) = -\kappa \boldsymbol{J}(\boldsymbol{r}, t) \cdot \boldsymbol{\nabla} V(\boldsymbol{r}) + D\nabla^2 T(\boldsymbol{r}, t). \tag{3}$$

*michael.jack@otago.ac.nz

The first term on the right-hand side represents the heat transfer from the Brownian system to the environment and the second term represents heat diffusion. In Eq. (3), κ is proportional to the inverse of the heat capacity of the environment and D is the thermal diffusivity of the environment, which we have taken to be constant for simplicity. The coupled system given by Eqs. (1) and (3) defines the total system of interest in this paper. Equation (3) describes an environment that can be approximated as an incompressible fluid. Other choices for the equation of motion for the local environment are possible, but will not be considered here. In the remainder of the paper, we will explore the dynamics and thermodynamics of this system of coupled equations.

A similar model was discussed earlier by Streater [41–44] in the context of a Brownian particle. The current work goes beyond this to explore the consequences of self-induced temperature gradients on the dynamics of Brownian systems, including analytical and numerical calculations of the steady-state solution, numerical results for barrier-crossing rates, and a proposal for a heat engine and heat pump utilizing self-induced temperature gradients.

This article is arranged as follows. In Sec. II, we consider the relationship between self-induced temperature gradients and the first and second laws of thermodynamics. In Sec. III, we discuss the steady-state behavior of Eqs. (1) and (3). In Sec. IV, we determine dimensionless forms of Eqs. (1) and (3) and define two dimensionless parameters that determine the behavior of the system. In Sec. V, we describe a numerical technique for solving the dynamic forms of Eqs. (1) and (3) based on the finite-volume method. In Sec. VI, we explore the consequences of self-induced temperature gradients on a number of canonical potentials. In particular, we show how self-induced temperature gradients can affect barrier-crossing rates. In Sec. VII, we implement a heat pump–heat engine that utilizes self-induced temperature gradients. Section VIII concludes the paper.

II. THERMODYNAMICS OF SELF-INDUCED TEMPERATURE GRADIENTS

In this section, we describe the first and second laws of thermodynamics for a Brownian system governed by Eqs. (1) and (3). The total energy of the combined Brownian system and its environment is given by [43]

$$U(t) = \int_\Omega d\boldsymbol{r}\, P(\boldsymbol{r}, t) V(\boldsymbol{r}) + c_p \rho \int_\Omega d\boldsymbol{r}\, T(\boldsymbol{r}, t), \quad (4)$$

where the integral is over the region of interest Ω, ρ is the density, and c_p is the specific-heat capacity of the fluid environment at constant pressure. The first term is the potential energy of the system and the second is the thermal energy of the local environment treated as an incompressible fluid.

Differentiating Eq. (4) with respect to time, we have

$$\frac{dU(t)}{dt} = \int_\Omega d\boldsymbol{r}\, \partial_t P(\boldsymbol{r}, t) V(\boldsymbol{r}) + c_p \rho \int_\Omega d\boldsymbol{r}\, \partial_t T(\boldsymbol{r}, t). \quad (5)$$

Inserting Eqs. (1) and (3) and using integration by parts, we derive

$$\frac{dU(t)}{dt} = (1 - c_p \rho \kappa) \int_\Omega d\boldsymbol{r}\, \boldsymbol{J}(\boldsymbol{r}, t) \cdot \nabla V(\boldsymbol{r}) + B^W(t) + B^Q(t), \quad (6)$$

where

$$B^W(t) \equiv - \int_\Omega d\boldsymbol{r}\, \nabla \cdot [\boldsymbol{J}(\boldsymbol{r}, t) V(\boldsymbol{r})], \quad (7)$$

$$B^Q(t) \equiv c_p \rho D \int_\Omega d\boldsymbol{r}\, \nabla^2 T(\boldsymbol{r}, t). \quad (8)$$

$B^W(t)$ and $B^Q(t)$ represent flows of energy through the boundary of the system. For energy conservation, the first term in Eq. (6) must vanish, requiring

$$\kappa = \frac{1}{c_p \rho}. \quad (9)$$

The total entropy of the system is given by [43]

$$S(t) = -k_B \int_\Omega d\boldsymbol{r}\, P(\boldsymbol{r}, t) \ln[P(\boldsymbol{r}, t)]$$
$$+ c_p \rho \int_\Omega d\boldsymbol{r}\, \ln[T(\boldsymbol{r}, t)]. \quad (10)$$

The first term is the Shannon entropy [45] of the Brownian system and the second is the entropy of an incompressible fluid. Differentiating Eq. (10) with respect to time, we find

$$\frac{dS(t)}{dt} = -k_B \int_\Omega d\boldsymbol{r}\, \{\ln[P(\boldsymbol{r}, t)] + 1\} \partial_t P(\boldsymbol{r}, t)$$
$$+ c_p \rho \int_\Omega d\boldsymbol{r}\, \frac{\partial_t T(\boldsymbol{r}, t)}{T(\boldsymbol{r}, t)}. \quad (11)$$

Inserting Eqs. (1) and (3) and using integration by parts, we can write the second law of thermodynamics as

$$\frac{dS(t)}{dt} = \dot{S}^{\text{gen}}(t) + \mathcal{B}^J(t) + \mathcal{B}^Q(t), \quad (12)$$

where we have defined

$$\dot{S}^{\text{gen}}(t) \equiv \sum_j \gamma_j \int_\Omega d\boldsymbol{r}\, \frac{J_j(\boldsymbol{r}, t)^2}{T(\boldsymbol{r}, t) P(\boldsymbol{r}, t)}$$
$$+ c_p \rho D \int_\Omega d\boldsymbol{r} \left[\frac{\nabla T(\boldsymbol{r}, t)}{T(\boldsymbol{r}, t)} \right]^2 \quad (13)$$

and

$$\mathcal{B}^J(t) \equiv k_B \sum_j \left\{ \int_\Omega d\boldsymbol{r}\, \partial_j J_j(\boldsymbol{r}, t) \right.$$
$$\left. + \int_\Omega d\boldsymbol{r}\, \partial_j [J_j(\boldsymbol{r}, t) \ln P(\boldsymbol{r}, t)] \right\}, \quad (14)$$

$$\mathcal{B}^Q(t) \equiv c_p \rho D \int_\Omega d\boldsymbol{r}\, \nabla \cdot \left[\frac{\nabla T(\boldsymbol{r}, t)}{T(\boldsymbol{r}, t)} \right]. \quad (15)$$

$\mathcal{B}^J(t)$ and $\mathcal{B}^Q(t)$ are boundary terms representing the flow of entropy through the boundaries. $\dot{S}^{\text{gen}}(t)$ is a purely positive quantity which we can recognize as the rate of entropy generation inside the boundaries of the system. These derivations

show that Eqs. (1) and (3) in combination with Eq. (9) describe a thermodynamically consistent system.

Previous treatments of Brownian systems have focused only on the dynamics of the system itself [34,45]. Here, we consider Brownian dynamics plus the local environment. In other words, we have explicitly included the energy and entropy of the local environment in our treatment.

The physical origin of Eq. (9) can be understood from a closer inspection of the first term on the right-hand side of Eq. (6). This term represents the sum of the heat emitted by the Brownian system into the local environment (the only consideration in previous treatments) and the heat absorbed by the local environment. If energy is conserved, these heat flows must be equal and this term must vanish. $B^W(t)$ is familiar from previous treatments and represents the external work done on the Brownian system at the boundary. $B^Q(t)$ can be recognized as the heat flowing in through the boundary. Similarly, $\mathcal{B}^J(t)$ is the inward flow of entropy due to the probability current of the Brownian system itself, while $\mathcal{B}^Q(t)$ is the inward flow of entropy due to temperature gradients. The entropy generation $\dot{S}^{\text{gen}}(t)$ [Eq. (13)] is composed of two positive terms. The first term is familiar from constant-temperature situations [34] and vanishes only in the case of vanishing probability current. The second arises from the usual treatment of temperature gradients in the local environment.

It is clear that the boundary conditions of the system have important implications for the physics of these systems. For example, consider the case of a confining potential: $V(\mathbf{r})|_{\partial\Omega} \to \infty$, $P(\mathbf{r},t)|_{\partial\Omega} = 0$, and $J(\mathbf{r},t)|_{\partial\Omega} = 0$. In this case, no work can be done by the system, $B^W(t) = 0$, and entropy flow is also zero, $\mathcal{B}^J(t) = 0$. This is familiar from the treatment of isothermal systems. In the current case, the boundary values of $T(\mathbf{r},t)$ and/or its derivatives must also be specified. If $\nabla T(\mathbf{r},t)|_{\partial\Omega} = 0$, then there is no heat flow at the boundaries, so $B^Q(t) = 0$. In this case, the system plus local environment system are thermally insulated from the greater environment. Other possible boundary conditions will be discussed below.

III. STEADY STATE

In the steady state, $\partial_t P(\mathbf{r},t) = 0$ and $\partial_t T(\mathbf{r},t) = 0$, we find that Eqs. (1) and (3) reduce to

$$\nabla \cdot \mathbf{J}_{\text{ss}}(\mathbf{r}) = 0, \tag{16}$$

$$\nabla \cdot \left[-\frac{1}{c_p \rho} \mathbf{J}_{\text{ss}}(\mathbf{r}) V(\mathbf{r}) + D \nabla T_{\text{ss}}(\mathbf{r}) \right] = 0. \tag{17}$$

The first equation states that the probability current in the steady state is a divergence-free field and the second expresses the local conservation of energy. In the steady state, the first [Eq. (6)] and second [Eq. (12)] laws of thermodynamics become

$$B_{\text{ss}}^W + B_{\text{ss}}^Q = 0, \tag{18}$$

$$\dot{S}_{\text{ss}}^{\text{gen}} + \mathcal{B}_{\text{ss}}^J + \mathcal{B}_{\text{ss}}^Q = 0. \tag{19}$$

In the steady state, Eq. (18) is redundant as it is a special case of Eq. (17) that holds at the boundaries.

In the special case when $\mathbf{J}_{\text{ss}}(\mathbf{r}) = 0$ everywhere, the probability density is given by

$$P_{\text{ss}}(\mathbf{r}) \propto \exp\left\{ -\int^{\mathbf{r}} d\mathbf{r}' \frac{\nabla V(\mathbf{r}')}{k_B T_{\text{ss}}(\mathbf{r}')} \right\}. \tag{20}$$

In addition, $\mathbf{J}_{\text{ss}}(\mathbf{r}) = 0$ implies that $\mathcal{B}_{\text{ss}}^J$ vanishes and

$$\dot{S}_{\text{ss}}^{\text{gen}} = -\mathcal{B}_{\text{ss}}^Q = -c_p \rho D \int_{\Omega} d\mathbf{r} \nabla \cdot \left[\frac{\nabla T_{\text{ss}}(\mathbf{r})}{T_{\text{ss}}(\mathbf{r})} \right]. \tag{21}$$

If, in addition, there is no heat flow at the boundaries, i.e., $\nabla T_{\text{ss}}(\mathbf{r})|_{\partial\Omega} = 0$, then $\dot{S}_{\text{ss}}^{\text{gen}} = 0$, $T_{\text{ss}}(\mathbf{r}) = T_0$ is constant, and $P_{\text{ss}}(\mathbf{r}) \propto \exp\{-V(\mathbf{r})/k_B T_0\}$ has the familiar Boltzmann form.

The steady-state solution simplifies in one dimension. In this case, from Eq. (16), the current is constant, $J_{\text{ss}}(x) = J_{\text{ss}}$, and, by integrating Eq. (17) twice, we find

$$T_{\text{ss}}(x) = \frac{J_{\text{ss}}}{c_p \rho D} \int_0^x V(x')dx' + \xi x + d, \tag{22}$$

where ξ and d are constants. The steady-state probability density takes the form

$$P_{\text{ss}}(x) = \psi(x) \left[P_{\text{ss}}(0) - J_{\text{ss}} \int_0^x \frac{1}{k_B T_{\text{ss}}(y)\psi(y)} \, dy \right], \tag{23}$$

where $\psi(x) = \exp\left[-\int_0^x \frac{V'(y)}{k_B T_{\text{ss}}(y)} \, dy \right]$. Equations (22) and (23) can be solved self-consistently once boundary conditions have been specified. An example of this will be considered in Sec. VII.

A potential of interest to Brownian systems is a tilted periodic potential [31] of the form

$$V(\mathbf{r}) = V_0(\mathbf{r}) - \mathbf{f} \cdot \mathbf{r}, \tag{24}$$

where $V_0(\mathbf{r})$ is periodic. In the usual isothermal case, this potential results in a periodic steady-state probability and current [31]. However, due to the fact that we are explicitly treating the environment, we can arrive at very different results. Let us first consider the case of one dimension, $\mathbf{r} = (x)$, with a tilted periodic potential given by $V(x) = V_0(x) - fx$, where $V_0(x) = V_0(x + L)$. This case is quite constrained as both the Brownian system and its environment are restricted to one degree of freedom, which is reflected in the available solutions to Eqs. (16) and (17). From Eq. (22), we see that the tilt causes the temperature to grow as x^2. Obviously this is not compatible with a periodic $T_{\text{ss}}(x)$ or $P_{\text{ss}}(x)$. This thus contrasts with treatments of Brownian systems where the environment is not being treated explicitly [11]. The physical origin of this behavior is the limited degrees of freedom of the environment for heat dissipation. The Brownian system loses potential energy as it propagates down the potential. This lost energy is emitted as heat to the environment and since there is only one environmental degree of freedom, this causes the temperature to rise. From this observation, it is clear that a linear tilted potential in one dimension is only possible on a bounded domain. We consider this case in more detail in Secs. VI C and VII.

It is useful to consider the generality of the above result. We note that the above conclusion could also be reached by integrating Eq. (17) once over the region $x = 0$ to $x = L$. This

gives

$$D\{\partial_x T_{ss}(x)|_{x=L} - \partial_x T_{ss}(x)|_{x=0}\} = -\frac{1}{c_p \rho} J_{ss} f L, \quad (25)$$

showing that in general, in one dimension, the nonzero tilt and current give rise to an unbalanced heat flow from the region. Next let us consider a two-dimensional case, where the potential is confining in the y direction and a tilted periodic potential in the x direction: $V(x, y) = V_0(x, y) - fx$, where $V_0(x, y) = V_0(x + L, y)$ and $V_0(x, y = \pm l) \to \infty$. Due to the confining potential, $J_y^{ss}(x, y = \pm l) = 0$. Integrating Eq. (17) over the two-dimensional domain $y = -l$ to $y = l$ and $x = 0$ to $x = L$, we find

$$D \int_{-l}^{+l} dy\{\partial_x T_{ss}(x, y)|_{x=L} - \partial_x T_{ss}(x, y)|_{x=0}\}$$

$$+ D \int_0^L dx\{\partial_y T_{ss}(x, y)|_{y=+l} - \partial_y T_{ss}(x, y)|_{y=-l}\}$$

$$= -\frac{1}{c_p \rho} f L \int_{-l}^{+l} dy J_x^{ss}(L, y). \quad (26)$$

From this equation, we can deduce the following. For finite $J_x^{ss}(x, y)$ (i.e., current flowing down the tilted potential), it is possible for $T_{ss}(x, y)$ to be periodic in x (in which case the first term vanishes), and therefore it is possible for $P_{ss}(x, y)$ to be periodic in x, as long as the heat generated from the downhill motion can be dissipated in the y direction (i.e., second term on the left-hand side does not vanish). This suggests that the strong constraints that arise in one dimension as described above are not present in higher dimensions.

IV. DIMENSIONLESS PARAMETERS

It is illustrative to find the dimensionless form of Eqs. (1) and (3) and determine dimensionless parameters that define the physical regimes of this system. For simplicity, we assume that $\gamma_j = \gamma$ has the same value in all dimensions. Now let $\hat{\boldsymbol{r}} = \boldsymbol{r}/L$, where L is a characteristic length scale defined such that on average only one Brownian particle is contained in the volume L^n, where n is the dimension of the system. Also let $\hat{V}(\hat{\boldsymbol{r}}) = V(\hat{\boldsymbol{r}})/E_0$ and $\hat{T}(\hat{\boldsymbol{r}}, t) = k_B T(\hat{\boldsymbol{r}}, t)/E_0$, where E_0 is the energy scale of the potential barriers experienced by the particle. With these definitions, we can write

$$\partial_{\hat{t}} \hat{P}(\hat{\boldsymbol{r}}, \hat{t}) = -\hat{\boldsymbol{\nabla}} \cdot \hat{\boldsymbol{J}}(\hat{\boldsymbol{r}}, \hat{t}), \quad (27a)$$

$$\hat{\boldsymbol{J}}(\hat{\boldsymbol{r}}, \hat{t}) = -[\hat{P}(\hat{\boldsymbol{r}}, \hat{t})\hat{\boldsymbol{\nabla}}\hat{V}(\hat{\boldsymbol{r}}) + \hat{T}(\hat{\boldsymbol{r}}, \hat{t})\hat{\boldsymbol{\nabla}}\hat{P}(\hat{\boldsymbol{r}}, \hat{t})], \quad (27b)$$

and

$$\partial_{\hat{t}} \hat{T}(\hat{\boldsymbol{r}}, \hat{t}) = -A\hat{\boldsymbol{J}}(\hat{\boldsymbol{r}}, \hat{t}) \cdot \hat{\boldsymbol{\nabla}}\hat{V}(\hat{\boldsymbol{r}}) + B\hat{\nabla}^2\hat{T}(\hat{\boldsymbol{r}}, \hat{t}), \quad (28)$$

where we have also defined $\hat{P}(\hat{\boldsymbol{r}}, t) = L^n P(\hat{\boldsymbol{r}}, t)$ and $\hat{t} = \frac{E_0}{\gamma L^2}t$. In Eq. (28), we have introduced the dimensionless parameters

$$A \equiv \frac{k_B}{\rho c_p} \frac{1}{L^n} \quad (29)$$

and

$$B \equiv \frac{\gamma D}{E_0}. \quad (30)$$

If we think of L^n as the volume required to fit a single particle, then $1/L^n$ is the concentration of particles for a given environment. Therefore, one can interpret A^{-1} as the dimensionless heat capacity. On the other hand, B indicates how quickly temperature gradients dissipate with respect to the rate of evolution of the Brownian particle. To see this, notice that the Brownian particle will move more slowly with either increased E_0 or decreased γ. However, temperature gradients will diffuse more quickly for larger D.

If B is much larger than A, then any self-induced temperature gradients will quickly diffuse away. However, when A and B are of comparable magnitude, self-induced temperature gradients will significantly alter the dynamics and the steady state of the system. Now consider the limit $B \gg 1$ and $A \ll 1$ accompanied by boundary conditions $\hat{T}(\hat{\boldsymbol{r}})|_{\partial\Omega} = \hat{T}_0$. In this regime, self-induced temperature gradients rapidly decay and the heat produced by the particle is emitted through the boundary. To a good approximation, we can then put $\hat{T}(\hat{\boldsymbol{r}}, \hat{t}) = \hat{T}_0$ and the system reduces to the isothermal case.

In the remainder of this paper, analysis is carried out using the dimensionless equations (27) and (28), so we drop the hats for notational convenience.

V. NUMERICAL METHODS

The system of equations (27) and (28) represent a set of coupled nonlinear partial differential equations. Since no general analytical solution exists, numerical methods are required. In this section, we develop a numerical approach for solving the steady state and dynamical evolution of the system.

A. Numerical methods for dynamics

The numerical approach pursued here is the finite-volume method, which is suited to conservation equations [46]. Equation (28) is not in the form of a conservation equation, since the first term is a source term that cannot be written as the divergence of a vector field. However, as discussed in Sec. II, energy is a conserved property. This means that the energy density

$$u(\boldsymbol{r}, t) = P(\boldsymbol{r}, t)V(\boldsymbol{r}) + \frac{1}{A}T(\boldsymbol{r}, t) \quad (31)$$

evolves via

$$\partial_t u(\boldsymbol{r}, t) = -\boldsymbol{\nabla} \cdot \left[V(\boldsymbol{r})\boldsymbol{J}(\boldsymbol{r}, t) - \frac{B}{A}\boldsymbol{\nabla}T(\boldsymbol{r}, t)\right], \quad (32)$$

which is in the form of a conservation equation. We now have a set of two conservation equations (27) and (32) that we can solve numerically to find $P(\boldsymbol{r}, t)$ and $T(\boldsymbol{r}, t)$ [via Eq. (31)] as a function of time.

The numerical approach we use consists of discretizing Eqs. (27) and (32) in space via finite volumes and propagating the system forward in time using the method of lines [47]. We will explain this process in one spatial dimension; however, the same idea may be applied to multiple dimensions. We discretize using uniform spacing Δx with each grid point denoted with an index $i : i \in 1, 2, \ldots, N$, where N is the number of grid points. We have $x_i = x_0 + i\Delta x$, where x_0 is

the left boundary of the system. We also define $f_i = f(x_i)$ for any function of x. If we define

$$\bar{p}_i = \frac{1}{\Delta x} \int_{x_{i-1}}^{x_i} P(x)\, dx, \tag{33}$$

$$\bar{u}_i = \frac{1}{\Delta x} \int_{x_{i-1}}^{x_i} u(x)\, dx, \tag{34}$$

and

$$J_i = -[P_i(\partial_x V)_i + T_i(\partial_x P)_i], \tag{35}$$

$$K_i = J_i V_i - \frac{B}{A}(\partial_x T)_i, \tag{36}$$

then the discretized equations of motion become

$$\frac{d\bar{p}_i}{dt} = \frac{1}{\Delta x}\big[J_{i-\frac{1}{2}} - J_{i+\frac{1}{2}}\big], \tag{37}$$

$$\frac{d\bar{u}_i}{dt} = \frac{1}{\Delta x}\big[K_{i-\frac{1}{2}} - K_{i+\frac{1}{2}}\big]. \tag{38}$$

Evaluating the spatial derivatives $(\partial_x P)_i$ and $(\partial_x T)_i$ via finite differences, we get

$$\frac{d\bar{p}_i}{dt} = \frac{1}{\Delta x}\Bigg\{ \bar{p}_{i-1}\bigg[-\frac{(\partial_x V)_{i-\frac{1}{2}}}{2} + \frac{T_{i-1}+T_i}{2\Delta x} \bigg] $$
$$+ \bar{p}_i\bigg[-\frac{(\partial_x V)_{i-\frac{1}{2}} - (\partial_x V)_{i+\frac{1}{2}}}{2} - \frac{T_{i-1}+2T_i+T_{i+1}}{2\Delta x} \bigg]$$
$$+ \bar{p}_{i+1}\bigg[\frac{(\partial_x V)_{i+\frac{1}{2}}}{2} + \frac{T_{i+1}+T_i}{2\Delta x} \bigg] \Bigg\}, \tag{39}$$

$$\frac{d\bar{u}_i}{dt} = \frac{1}{\Delta x}\Bigg\{ -\bigg[\bar{p}_{i-\frac{1}{2}}(\partial_x V)_{i-\frac{1}{2}} + T_{i-\frac{1}{2}}\frac{\bar{p}_i - \bar{p}_{i-1}}{\Delta x} \bigg]V_{i-\frac{1}{2}}$$
$$+ \bigg[\bar{p}_{i+\frac{1}{2}}(\partial_x V)_{i+\frac{1}{2}} + T_{i+\frac{1}{2}}\frac{\bar{p}_{i+1} - \bar{p}_{i-1}}{\Delta x} \bigg]V_{i+\frac{1}{2}}$$
$$+ \frac{B}{A\Delta x}(T_{i-1} - 2T_i + T_{i+1}) \Bigg\}, \tag{40}$$

where from Eq. (31) we have

$$T_i = A(\bar{u}_i - \bar{p}_i V_i). \tag{41}$$

To simulate the system, at each time step we use Eqs. (39)–(41) to update $\bar{p}_i$, $\bar{u}_i$, and T_i, respectively. Given initial and boundary conditions, this set of equations can be solved numerically as a system of ordinary differential equations (ODEs) coupled to an algebraic equation.

B. Numerically calculating the steady state

Setting the left-hand side of Eqs. (37) and (38) to zero gives us a very natural way of finding the steady state of the system. We can also apply the boundary conditions to P and T directly, depending on the physical situation that we are modeling. One particular case of interest is the case where the probability density is periodic (and normalized), while the temperature is held fixed at both ends, so that $T_1 = T_l$ and $T_N = T_r$. An example of such a case is explored in Sec. VII. In order to

solve this problem, we have to solve $2N$ equations given by

$$J_{i-\frac{1}{2}} = J_{i+\frac{1}{2}} \quad \forall\, i \in 2,\ldots,N-2, \tag{42a}$$

$$K_{i-\frac{1}{2}} = K_{i+\frac{1}{2}} \quad \forall\, i \in 2,\ldots,N-2, \tag{42b}$$

$$\sum_{i=1}^{N} \bar{p}_i = \frac{1}{\Delta x}, \tag{42c}$$

$$\bar{p}_1 = \bar{p}_N, \tag{42d}$$

$$T_1 = T_l, \tag{42e}$$

$$T_N = T_r. \tag{42f}$$

Equations (42) are nonlinear in both P and T, so they cannot be written as a matrix equation. Instead, we must use iterative numerical techniques suited to nonlinear equations.

VI. SELF-INDUCED TEMPERATURE GRADIENTS AND BARRIER CROSSING

In this section, we consider the impact of self-induced temperature gradients on barrier crossing in one dimension. We consider three systems that are important to the topic of Brownian dynamics: the bistable well, the metastable well, and the tilted periodic potential.

A. Bistable well

The bistable well is a potential that has two states of equilibrium with an intermediate unstable maximum and is often used as a starting point for investigating systems in statistical mechanics [16,21]. In Ref. [35], Landauer used the bistable potential to show that an externally imposed nonuniform temperature can affect the relative occupation of states. Here we show that self-induced temperature gradients can affect a Brownian system in a similar fashion. We consider the potential

$$V(x) = -b\{\sinh(x) + a\ln[\cosh(x)] - c\,x^4\}, \tag{43}$$

where $a = 30$, $b = 0.08$, and $c = 1.5$ [see Fig. 1(a)]. The points of stability of $V(x)$ are located at $x_a \approx -2$ and $x_c \approx 2$, and the local maximum is at $x_b \approx 0$. We impose Neumann boundary conditions on the temperature so that no heat can escape through the boundaries ($\nabla T|_{\partial\Omega} = 0$), where $\Omega = [x_0 = -5, x_1 = 5]$. Since this is a confining potential and the total system is thermally insulated, the steady-state probability has the Boltzmann form $P_{ss}(x) = \mathcal{N}\exp[-V(x)/T_{ss}]$. The steady-state temperature T_{ss} can be found by invoking energy conservation [cf. Eq. (4)],

$$\int_{x_0}^{x_1} P(x,0)V(x)\,dx + \frac{1}{A}\int_{x_0}^{x_1} T(x,0)\,dx$$
$$= \mathcal{N}\int_{x_0}^{x_1} \exp\bigg[-\frac{V(x)}{T_{ss}}\bigg]V(x)\,dx + \frac{1}{A}(x_1 - x_0)T_{ss}. \tag{44}$$

The left-hand side is the initial energy of the Brownian system plus the energy of the environment at $t = 0$, while the right-hand side is the energy in the steady state. Note that the steady state does not depend on B in this zero current situation.

We can find the probability and temperature distribution at intermediate times by numerical solution of Eqs. (27) and (28),

FIG. 2. Evolution of $P_+(t)$ as a function of time. The (blue) solid line represents $A = 0$ (where Kramers rate is expected to hold), the (orange) dotted line represents $A = 0.5$, and the (green) dashed line represents $A = 1$. B is held fixed at 0.05. Note that the y axis is a logarithmic scale.
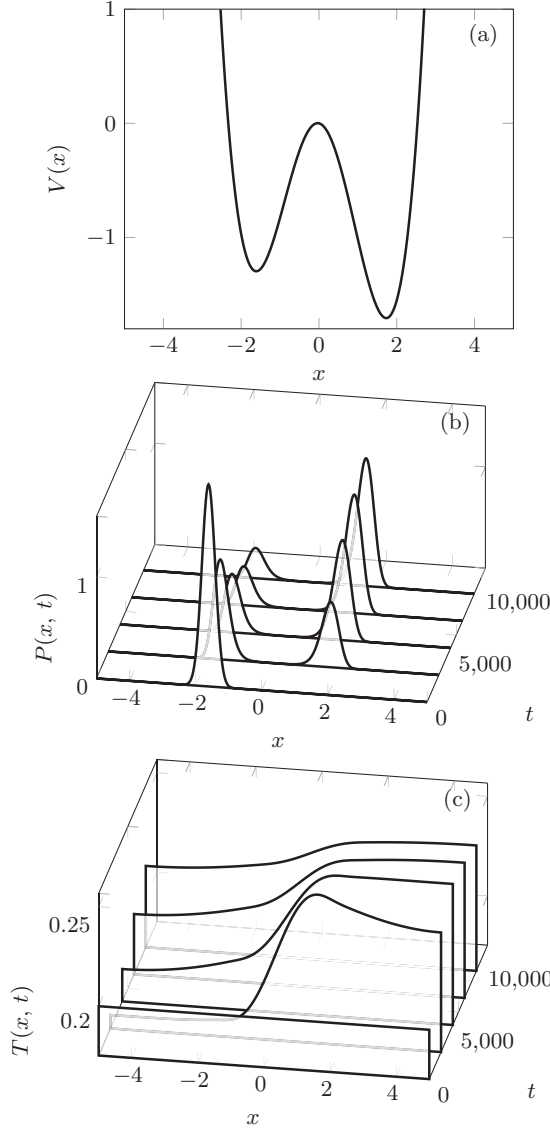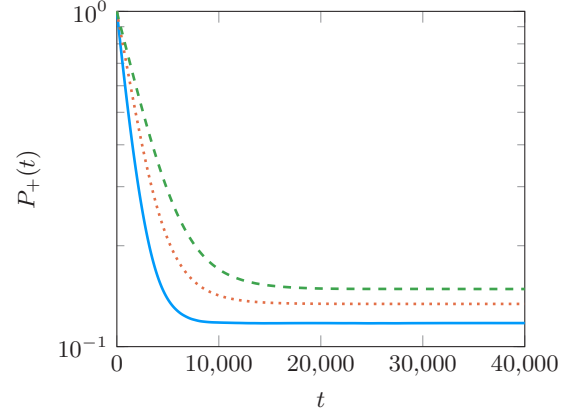

FIG. 1. Bistable potential. (a) Bistable well given by Eq. (43). (b) Probability as a function of time. (c) Temperature as a function of time. Simulation parameters are $B = 0.005$ and $A = 1$.

as discussed in Sec. V. We solve the relevant ODEs using the DIFFERENTIALEQUATIONS.JL [48] package in JULIA [49]; the relevant code can be found in the Supplemental Material [50].

The time evolution of a Brownian system initially in the left-hand well is shown in Figs. 1(b) and 1(c). As time proceeds, the initial constant temperature develops gradients and the upper well cools down, while the lower well heats up. Physically, this is because the Brownian system draws heat from the environment in order to surmount the barrier. For longer times, the temperature gradients disappear due to heat diffusion. In the final state, all of the potential energy has been converted into thermal energy in the environment.

It is common to describe a bistable system in the deep-well regime ($T \ll 1$ in our units) in terms of the probabilities of occupation in the two wells. We define the probability that the system is in the upper and lower well by $P_+(t) = \int_{x_0}^{x_b} dx\, P(x,t)$ and $P_-(t) = \int_{x_b}^{x_1} dx\, P(x,t)$, respectively. For

isothermal Brownian motion [$A = 0$ and $T(x,t) = T_0$], this deep-well limit is called Kramers regime. In Kramers regime, the probability $P_+(t)$ evolves as

$$\frac{dP_+(t)}{dt} = -r_+ P_+(t) + r_-[1 - P_+(t)], \quad (45)$$

where $r_+ = \frac{[V''(x_a)|V''(x_b)|]^{\frac{1}{2}}}{2\pi} e^{-[V(x_b)-V(x_a)]/T_0}$ and $r_- = \frac{[V''(x_c)|V''(x_b)|]^{\frac{1}{2}}}{2\pi} e^{-[V(x_b)-V(x_c)]/T_0}$ are the Kramers rates [20].

In the current case, with $A \neq 0$, the changing temperature distribution renders the above Kramers description invalid. Figure 2 shows the evolution of $P_+(t)$ for various different values of A and B calculated via the methods described in Sec. V. Figure 2 shows that larger A leads to slower decay and increased final population in the upper well. We can understand these results from the fact that when A is large, the potential energy that is converted into heat has a larger effect on the temperature of the environment. Therefore, for large A, the final temperature is increased, resulting in a larger probability of being excited to the upper well.

B. Decay from a metastable state

The second situation that we explore is escape over a barrier, as shown in Fig. 3 (a). Here we use the potential

$$V(x) = -b\{\sinh(x) + a\ln[\cosh(x)]\}, \quad (46)$$

where $a = 7$ and $b = 2$. Once a system manages to overcome the barrier at x_b, the potential rapidly decreases to $-\infty$ and the system will never return to x_a. For this system, if $A = 0$, then the Kramers deep-well regime applies. In this case, Eq. (45) holds with $r_- = 0$. Thus if the system is initially in the upper well [$P_+(t = 0) = 1$], then $P_+(t)$ will decay exponentially with time. On the other hand, when $A \neq 0$, self-induced temperature gradients render the Kramers description invalid and $P_+(t)$ will not decay exponentially. Figure 3(b) demonstrates the effect that B has on the barrier-crossing rate. In this figure, we have applied Dirichlet boundary conditions to the temperature so that the temperature at the boundaries
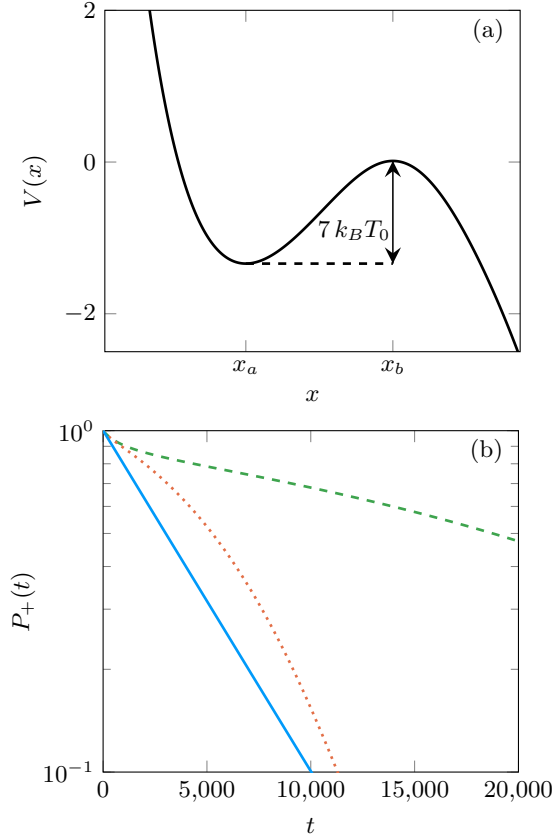
FIG. 3. (a) Metastable potential given by Eq. (46); T_0 is the initial temperature ($T_0 = 0.2$). (b) Logarithmic plot of the population in the upper well of a metastable potential $P_+(t)$ as a function of time. $P_+(t)$ is obtained by integrating the probability distribution over the interval $(-\infty, x_b]$. In all plots, $A = 0.5$, while the (blue) solid line $B = 10$, (orange) dotted line $B = 1 \times 10^{-3}$, and (green) dashed line $B = 1 \times 10^{-4}$.

remains constant. We set $A = 0.5$ and have plotted $P_+(t)$ for multiple values of B. In Fig. 3, we see that for smaller B, the barrier-crossing rate is reduced. When B is large, any temperature gradients that are produced will dissipate quickly and any excess heat will escape through the boundaries (since we have Dirichlet boundary conditions). Therefore, for large B, $P_+(t)$ decays exponentially, which is what we would have expected in the absence of self-induced temperature gradients. However, if B is small, then as the system crosses the barrier, the upper well will cool down, while the downwards slope to the right of x_b will heat up. Therefore, the temperature gradient will produce a force that opposes the crossing of the barrier. This effect of temperature gradients on barrier crossing is well known in terms of the blowtorch effect [35]; however, here the temperature gradient is self-induced.

C. Tilted periodic potential

The next situation that we consider is the tilted periodic potential on a finite domain. We consider the potential

$$V(x) = -0.2x + 0.8 \sin(2\pi x) + 4 \qquad (47)$$

[see Fig. 4(a)] and the initial state $P(x, 0) = (2\pi\sigma^2)^{-1/2} \exp(-x^2/2\sigma^2)$, where $\sigma = 0.2$, $T(x, 0) = 0.4$, and the
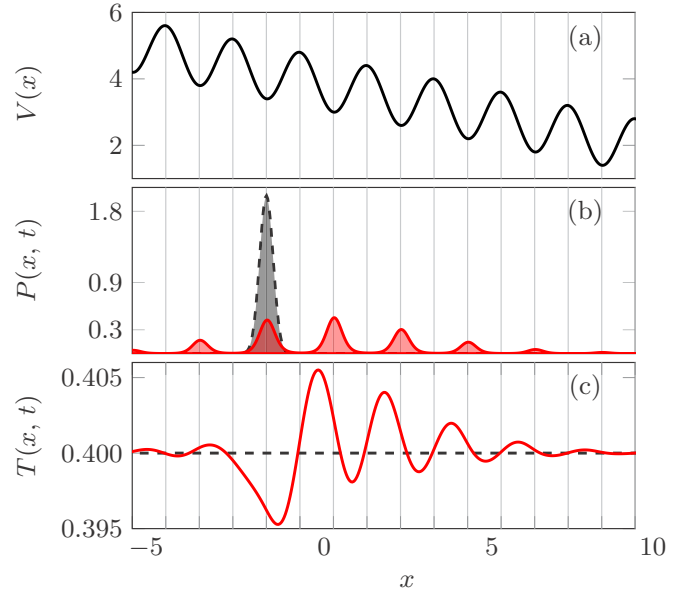

FIG. 4. Time evolution on a tilted periodic potential. (a) The tilted periodic potential given by Eq. (47). (b) The probability density. (c) The temperature in the tilted periodic potential. In both (b) and (c), the (black) dashed line represents $t = 0$ and the (red) solid line represents $t = 50.0$. The system parameters are $A = 0.01$ and $B = 0.005$.

temperature at the boundaries is held fixed (Dirichlet boundary conditions). The resulting time evolution of $P(x, t)$ and $T(x, t)$ is shown in Figs. 4(b) and 4(c), respectively. After some time, the system has diffused and moved down the potential. As the system diffuses down the potential, it produces oscillations in the temperature that are out of phase with the oscillations of the potential. A similar phenomena was discussed in Ref. [23], where it was pointed out that an externally imposed temperature oscillating out of phase with the potential will result in a net force. Here we see the inverse effect, where a Brownian system subject to a net force in a periodic potential causes the temperature to oscillate out of phase with potential. As before, for small B, the temperature gradients tend to resist the drift of the system down the potential. However, for large B, the temperature remains flat and the situation is reduced to the isothermal case.

The examples in this section all display similar behavior. Namely, when a Brownian system descends down a potential, it will emit heat into its environment. Also, as the system surmounts an energy barrier, it absorbs heat from the environment. If the temperature gradients caused by the heat exchanges do not diffuse away quickly, then the net motion of the Brownian system over the barrier will be reduced.

VII. IMPLEMENTATION OF A HEAT ENGINE AND HEAT PUMP

Brownian systems have been shown to work as heat engines and heat pumps [29,34,38,40,51–53] and a Brownian Carnot engine has been experimentally realized in [54]. In this section, we demonstrate how a Brownian system coupled to its local environment can act as a heat engine and heat pump operating between two spatially separated heat baths (refrigerators are
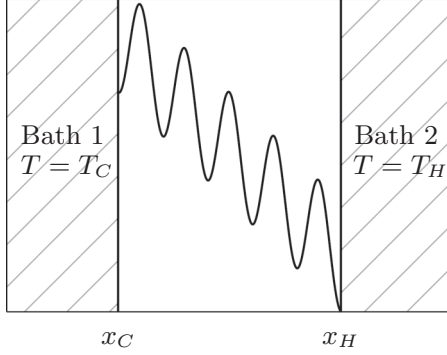
FIG. 5. Schematic of the heat engine or heat pump system with potential $V(x) = -fx + \sin(2\pi x)$. The temperature is held fixed at the boundaries: $T(x_C,t) = T_C$ and $T(x_H,t) = T_H$.

physically equivalent to heat pumps so will not be considered separately here).

Let us consider a finite domain $x \in [x_C, x_H]$ and impose Dirichlet boundary conditions on the temperature, such that $T(x_C, t) = T_C$ is the cold reservoir and $T(x_H, t) = T_H > T_C$ is the hot reservoir. For the potential, we will use the tilted periodic potential of the form depicted in Fig. 5. Finally, we impose periodic boundary conditions on the probability density: $P(x_C, t) = P(x_H, t)$. Physically, this boundary condition means that a system reaching one side of the barrier is immediately transported to the other side. The steady state of the system has a constant current J_{ss}, so Eqs. (22) and (23) hold.

The steady-state first law of thermodynamics for the system can be written as $\dot{W} - \dot{Q}_C - \dot{Q}_H = 0$ [cf. Eq. (18)], where $\dot{W} = J_{ss}\Delta V$ is the rate of work done by the system and $\dot{Q}_H = -\frac{B}{A} \partial_x T(x)|_{x=x_H}$ and $\dot{Q}_C = \frac{B}{A} \partial_x T(x)|_{x=x_C}$ are the rate of heat from the hot reservoir and cold reservoir, respectively. Here, $\Delta V = -f(x_H - x_C)$, where f is the tilt. The system can operate in a number of regimes: as a heat engine, $\dot{Q}_H > 0$ and $\dot{W} > 0$, where the first-law efficiency is $\eta_{\mathrm{I}}^{\mathrm{HE}} = \dot{W}/\dot{Q}_H$, and as a heat pump, $\dot{Q}_H < 0$, $\dot{Q}_C > 0$, and $\dot{W} < 0$, where the first-law efficiency, or coefficient of performance (COP), is $\eta_{\mathrm{I}}^{\mathrm{HP}} = \dot{Q}_H/\dot{W}$. The steady-state second law of thermodynamics for the system can be written as $\dot{S}_{ss}^{\mathrm{gen}} = -\dot{Q}_C/T_C - \dot{Q}_H/T_H \geqslant 0$ [cf. Eq. (21)], which means that, as expected, both heat-engine and heat-pump efficiencies are constrained by the Carnot efficiency. We can therefore define the second-law efficiency for these two systems as [34]

$$\eta_{\mathrm{II}}^{\mathrm{HE}} = \eta_{\mathrm{I}}^{\mathrm{HE}}\left(1 - \frac{T_C}{T_H}\right)^{-1}, \tag{48a}$$

$$\eta_{\mathrm{II}}^{\mathrm{HP}} = \eta_{\mathrm{I}}^{\mathrm{HP}}\left(1 - \frac{T_C}{T_H}\right), \tag{48b}$$

where both efficiencies $\eta_{\mathrm{II}}^{\mathrm{HE}}$ and $\eta_{\mathrm{II}}^{\mathrm{HP}}$ are now bounded by 1.

We can determine the efficiency as a function of the parameters by solving for J_{ss} using the methods described in Sec. V B. The equations were solved by reformulating the problem as an optimization problem and using the JUMP.JL [55] package in JULIA; the code can be found in the Supplemental Material [50].
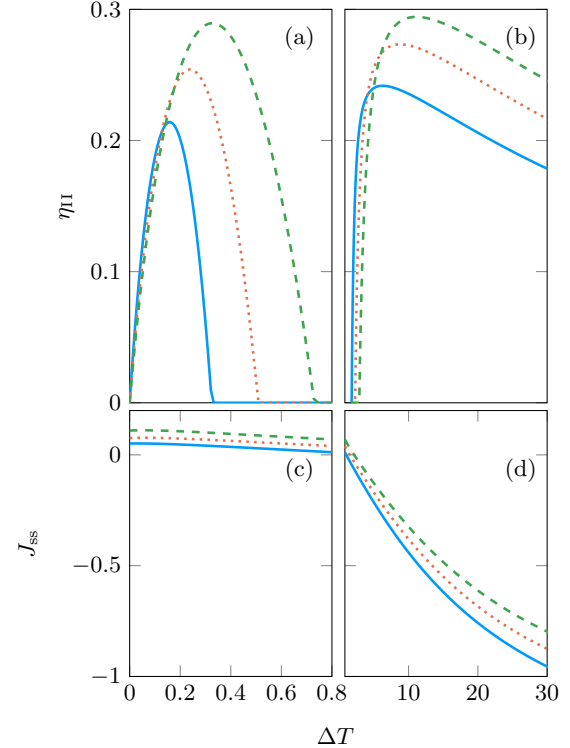

FIG. 6. We use the potential of Fig. 5 to explore the second-law efficiency of the system as a function of $\Delta T \equiv T_H - T_C$, where $T_C = 0.5$. (a) The efficiency for small ΔT where the system behaves as a heat pump. (b) The efficiency for large ΔT where the large-temperature gradients cause the system to act as a heat engine. (c),(d) The steady-state current J_{ss} as a function of ΔT. The (blue) solid line represents a tilt of $f = 0.6$, the (orange) dotted line represents $f = 1$, and the (green) dashed line represents $f = 3$.

In Figs. 6(a) and 6(b), we plot the efficiency of the system as a function of $\Delta T \equiv T_H - T_C$ for multiple values of the force f. For $\Delta T < 1$, the system behaves as a heat pump. In this case, the current flow is down the slope of the potential [$J_{ss} > 0$; see Fig. 6(c)]. When ΔT is small, the system emits heat into the hot bath, while drawing heat from the cold bath. However, as ΔT increases, the dominant heat flow is the flow due to diffusion [second term on the right-hand side of Eq. (28)]. In this case, the temperature will simply become a straight line from T_C at $x = x_C$ to T_H at $x = x_H$. In this case, the system behaves as a loss process. At around $\Delta T = 1$, the temperature gradients cause the current to flow against the slope of the potential [$J_{ss} < 0$; see Fig. 6(d)]. In this case, the system is doing work and acts as a heat engine. As ΔT increases further, $\dot{Q}_H$ increases and the heat-engine efficiency goes to zero.

VIII. CONCLUSIONS

We have carried out a theoretical investigation of a Brownian system dynamically coupled via heat exchanges to its local environment. The composite system is described by an equation for the probability distribution of the Brownian subsystem with a spatially dependent temperature [Eq. (27)] and one for the temperature of the local environment with a

heat-source term due to the Brownian subsystem [Eq. (28)]. We have defined two dimensionless parameters, A and B, characterizing the physical regimes of the system, where A can be interpreted as the inverse of the effective heat capacity of the environment and B as the relative rate of dissipation of temperature in the environment. If $B \gg 1$ and $A \ll 1$, the system reduces to the well-known isothermal case [5,31–34]. Outside of this regime, the dynamics and thermodynamics of the system differ significantly from the isothermal case.

The relaxation of the Brownian subsystem to its steady state is found to be strongly dependent on the degrees of freedom and the boundary conditions of the local environment. For example, consider the tilted periodic potential, where the system and local environment are restricted to one degree of freedom [31]. If one includes self-induced temperature gradients, then the heat emitted as the system propagates down the potential causes the environmental temperature to rise without limit. This does not occur if there are other degrees of freedom available for heat dissipation.

We have developed a method to numerically solve the two nonlinearly coupled partial differential equations (27) and (28), describing the composite system. The approach is based on the finite-volume method and exploits a reformulation as conservative equations. The numerical method is used to explore a number of barrier-crossing scenarios in one dimension. A Brownian system absorbs heat from the environment to surmount a barrier and loses heat as it descends.

Our calculations show how the temperature gradients caused by these flows of heat influence the barrier-crossing rates. In particular, for $A \neq 0$ and $B \ll 1$, barrier-crossing rates are significantly reduced by slowly diffusing self-induced temperature gradients. In addition, in the deep-well regime, the decay behavior differs from the commonly used Kramers description [20].

Finally, we have demonstrated a realization of a heat pump and heat engine by a Brownian system with self-induced temperature gradients in its local environment. This system has two spatially separated heat baths and a specially constructed tilted potential. It can operate as a heat pump or as a heat engine, depending on the temperature difference between the two baths. Efficiencies of the system in both regimes were calculated and shown to be limited by the Carnot efficiency, as expected.

In this paper, we have focused on the overdamped regime. It has been argued that the transfer of heat from a Brownian system to its environment is dominated by kinetic energy [26–28]. Generalization of this work to include inertia would be an interesting topic for future work.

[1] C. Gardiner, in *Stochastic Methods*, edited by H. Haken (Springer, Berlin, 2009).

[2] J. D. Bryngelson and P. G. Wolynes, J. Phys. Chem. **93**, 6902 (1989).

[3] S. Leibler and D. A. Huse, C. R. Acad. Sci. III **313**, 27 (1991).

[4] S. Leibler and D. A. Huse, J. Cell Biol. **121**, 1357 (1993).

[5] D. Keller and C. Bustamante, Biophys. J. **78**, 541 (2000).

[6] M. J. Tyska and D. M. Warshaw, Cell Motil. Cytoskeleton **51**, 1 (2002).

[7] R. D. Astumian and P. Hanggi, Phys. Today **55**, 33 (2002).

[8] R. Phillips and S. R. Quake, Phys. Today **59**, 38 (2006).

[9] R. D. Astumian, Phys. Chem. Chem. Phys. **9**, 5067 (2007).

[10] I. Santamaría-Holek, A. Gadomski, and J. Rubi, J. Phys.: Condens. Matter **23**, 235101 (2011).

[11] X.-g. Ma, Y. Su, P.-Y. Lai, and P. Tong, Phys. Rev. E **96**, 012601 (2017).

[12] Z. Wang, Biointerphases **5**, FA63 (2010).

[13] M. von Delius, E. M. Geertsema, D. A. Leigh, and D.-T. D. Tang, J. Am. Chem. Soc. **132**, 16134 (2010).

[14] M. von Delius, E. M. Geertsema, and D. A. Leigh, Nat. Chem. **2**, 96 (2010).

[15] P. A. Quinto-Su, Nat. Commun. **5**, 5889 (2014).

[16] C. J. Myers, M. Celebrano, and M. Krishnan, Nat. Nanotechnol. **10**, 886 (2015).

[17] V. Blickle and C. Bechinger, Nat. Phys. **8**, 143 (2012).

[18] G. E. Uhlenbeck and L. S. Ornstein, Phys. Rev. **36**, 823 (1930).

[19] H. Eyring, J. Chem. Phys. **3**, 107 (1935).

[20] H. A. Kramers, Physica **7**, 284 (1940).

[21] R. Landauer, IBM J. Res. Dev. **5**, 183 (1961).

[22] R. P. Feynman, in *Feynman Lectures on Physics*, edited by M. Gotteib (California Institute of Technology, Pasadena, CA, 1963).

[23] M. Büttiker, Z. Phys. B **68**, 161 (1987).

[24] N. van Kampen, J. Math. Phys. **29**, 1220 (1988).

[25] J. M. R. Parrondo and P. Español, Am. J. Phys. **64**, 1125 (1996).

[26] K. Sekimoto, J. Phys. Soc. Jpn. **66**, 1234 (1997).

[27] K. Sekimoto, Prog. Theor. Phys. Suppl. **130**, 17 (1998).

[28] T. Hondou and K. Sekimoto, Phys. Rev. E **62**, 6021 (2000).

[29] R. Benjamin and R. Kawai, Phys. Rev. E **77**, 051132 (2008).

[30] P. Reimann, Phys. Rep. **361**, 57 (2002).

[31] D. Cubero and F. Renzoni, *Brownian Ratchets: From Statistical Physics to Bio and Nano-Motors* (Cambridge University Press, Cambridge, 2016).

[32] M. O. Magnasco, Phys. Rev. Lett. **72**, 2656 (1994).

[33] K. J. Challis and M. W. Jack, Phys. Rev. E **88**, 042114 (2013).

[34] M. W. Jack and C. Tumlin, Phys. Rev. E **93**, 052109 (2016).

[35] R. Landauer, J. Stat. Phys. **53**, 233 (1988).

[36] M. O. Magnasco and G. Stolovitzky, J. Stat. Phys. **93**, 615 (1998).

[37] C. Bustamante, J. Liphardt, and F. Ritort, Phys. Today **58**, 43 (2005).

[38] N. Nakagawa and T. S. Komatsu, Europhys. Lett. **75**, 22 (2006).

[39] V. Blickle, T. Speck, L. Helden, U. Seifert, and C. Bechinger, Phys. Rev. Lett. **96**, 070603 (2006).

[40] M. Das, D. Das, D. Barik, and D. S. Ray, Phys. Rev. E **92**, 052102 (2015).

[41] R. Streater, J. Math. Phys. **38**, 4570 (1997).

[42] R. Streater, J. Stat. Phys. **88**, 447 (1997).

[43] R. Streater, Rep. Math. Phys. **40**, 557 (1997).

[44] R. F. Streater, Proc. R. Soc. London, Ser. A **456**, 205 (2000).

[45] C. Van den Broeck and M. Esposito, Phys. Rev. E **82**, 011144 (2010).

[46] R. J. LeVeque, *Finite Volume Methods for Hyperbolic Problems* (Cambridge University Press, Cambridge, 2002), Vol. 31.

[47] W. E. Schiesser, *The Numerical Method of Lines: Integration of Partial Differential Equations* (Elsevier, Amsterdam, 2012).

[48] C. Rackauckas and Q. Nie, J. Open Res. Softw. **5**, 15 (2017).

[49] J. Bezanson, A. Edelman, S. Karpinski, and V. B. Shah, SIAM Rev. **59**, 65 (2017).

[50] See Supplemental Material at http://link.aps.org/supplemental/10.1103/PhysRevE.96.062130 for implementations of the numerical methods.

[51] C. Jarzynski and O. Mazonka, Phys. Rev. E **59**, 6448 (1999).

[52] C. Van den Broeck and R. Kawai, Phys. Rev. Lett. **96**, 210601 (2006).

[53] M. Hoshina and K. Okuda, Eur. Phys. J. B **90**, 78 (2017).

[54] I. A. Martínez, É. Roldán, L. Dinis, D. Petrov, J. M. Parrondo, and R. A. Rica, Nat. Phys. **12**, 67 (2016).

[55] I. Dunning, J. Huchette, and M. Lubin, SIAM Rev. **59**, 295 (2017).